A Numerical Study on Phonon-Phonon Interaction

Er. Birendra Jha
Senior Lecturer,
Government Polytechnic, Siwan, Bihar

Abstract- *The interaction of phonons with other phonons is an extremely important scattering mechanism in most semiconducting material. This scattering mechanism is vital in describing two thermal properties of system such as the mean-free path of the phonons and the thermal conductivity. Generally, Phonon interactions occur due to the enharmonic regime of the crystal potential and because of this it is possible for phonons to be created and destroyed via these interactions. In the present study, we discussed about the phonon-phonon interactions, which is the study of the lifetime of phonon modes. The results show that the relaxation rate of a phonon mode (that is the rate at which phonons interact) is equal to the inverse of the phonon mode's lifetime, which includes three-phonon interactions based on the dispersion relation. A detailed derivation of the three-phonon scattering relaxation rate is presented in this paper. A qualitative analytic expression for the relaxation rate of all acoustic phonon modes and an exact analytic expression for the decay rate of the two zone-center optical modes, in nanostructures are also derived.These results also discuss the importance of particular phonon branches in the relaxation rates of the phonon modes and what effects α change in the size of temperature of the nanotube have on the relaxation rate.*

Keywords- Phonons, interaction, theory, scattering, semiconductor, nanostructure

I. INTRODUCTION

Phonon-phonon interactions can be viewed as a perturbation on the harmonic system [1]. As this perturbation is small, these interactions can be described using Fermi's Golden Rule [2]. From the Golden Rule, one can calculate the lifetime of a phonon mode as a function of temperature. The theory of phonon-phonon interactions has been studied for over half a century. The theoretical treatment of these interactions is linked to the modelling of the enharmonic potential, a complicated and difficult term which can be approximately determined using second-order and third-order elastic constants, which are exceptionally hard to measure experimentally. This applies especially for nanostructures. As such, there have been several different approaches to modeling these interactions in bulk materials, but only recently has there been any progress in nanostructures [3,4]. In 1954, Herring was the among the first to use a relaxation time approach to understand and explore these interactions in bulk materials [5]. In his approach, based loosely on Fermi's Golden Rule, and the linear Debye relations), he showed that the relaxation rate of phonon modes undergoing three-phonon processes was directly proportional to the temperature [6]. However, this approach relies on the condition that the temperature is higher than the Debye temperature and uses a simplified form for the potential cubic enharmonic term v3. This relaxation time approach was adopted by Liebfried and Schlomann who had previously developed an enharmonic potential as part of their specific heat calculations in 1952 [7,8]. This enharmonic potential was calculated using a Debye-like continuum approach to modeling the potential. Using their potential, were able to calculate the lifetime of the acoustic phonon modes undergoing three-phonon interactions for bulk semiconductors. This potential was advantageous in that it had only one adjustable parameter, but was disadvantageous in that it required linear dispersion relations. This theory was then applied to several semiconductors and showed good agreement with experiment though in result it was a necessity to vary at learnt one adjustable parameter with temperature to match high and low temperature experimental results. Klemens, in 1958, proposed a second form for the enharmonic potential in bulk which also only applied in the long wavelength limit to acoustic phonons, by applying symmetry arguments [9-11]. The advantage of Klemens potential was that it applied to non-linear dispersion curves, which is the case in most real systems. The disadvantage of this potential was that it required one to have knowledge of the average velocity of the phonon modes (with no clear definition of how to calculate this) and had two scalable parameters. Also, Klemen's expression, like Leibfried's, had an arbitrary coupling between the interacting phonon modes. However, Klemens and Liebfrieds models did not agree on the low temperature relaxation rates. Later, in 1966 Klemens improved and generalized this potential and the resultant expression for the relaxation rate of phonon modes by including the effects of optical modes, but still the two theories could not agree [12]. Hamilton and Parrott in 1988, re-adapted and improved the form of the Leibfried's potential by expanding the potential in terms of the isotropic continuum model based upon the relations derived by Landau and Lifschitz [13-15]. By applying this approach, they showed that these scattering processes could explain the thermal conductance of germanium as a function of temperature using the Vibrational

Principle. Later, on this basis, Parrott applied this potential using the knowledge gained from the variastional approach to a Relaxation time approach. In 1994, Srivastava presented a detailed description of the relaxation rate of phonon modes [16-17]. Previous arbitrary parameters and coupling constants were replaced with measurable quantities and a clear description of the difference between Class 1 and Class 2 events was presented (Class 1, Class 2 events and Normal and Umklapp processes are defined in the following section). Also, by removing arbitrary coupling parameters, Srivastava was able to shoe that at high temperatures, Umklapp processes would dominate in bulk materials and at low temperature Normal processes would dominate. In his approach, he was able to discuss the exact contributions from different phonon modes, and only applied one semi-adjustable parameter, the Griineisen constant, which did not need to change with temperature. Later, in 1996, Srivastava improved upon the potential which Parrott had applied by re-moving the necessity to use linear dispersion relations and correcting the potential to show a similar form to that of Klemens, but with only one semi-adjustable parameter (the Gruneisin constant) and no arbitrary coupling factor. Later, by applying this relaxation time approach to germanium, Srivastava showed excellent agreement with experiment and explained the thermal conductivity in all regimes [16,18-21]. This included the high temperature regime which is dominated completely by three-phonon events. In 2011, Lax et al. showed, using momentum and energy conservation conditions, that certain decay routes of phonon modes (such as a high energy transverse acoustic phonon mode decaying into two lower energy transverse acoustic phonon modes) were impossible due to momentum and energy conservation conditions [22-23]. These conditions have been shown to apply to linear systems and also near the Brillouin zone center for non-linear systems where the dispersion curves are approximately linear. This is especially interesting when one considers nanotubes.

1.1. General expression

Here a clear derivation of the lifetime of three-phonon processes for selected phonon modes are presented. The expression for the lifetime of phonon modes is formulated for a one-dimensional system, whilst the three-dimensional approach is also given to enable direct comparison. Such a derivation is very complicated and as such some simplifications are used, though these are kept to a minimum. These expressions are derived based upon an approach known as the single mode relaxation time method (smrt). In this approach on assumes that all modes except the scattered are populated according to their Bose-Einstein equilibrium distribution [24-25]. The three-phonon scattering lifetime is calculated using Fermi's Golden Rule. Fermi's Golden Rule describes the transition probability $P_{i\to f}$ of an event as where Ei and Ef are the initial and final energy state of the system respectively, $|i\rangle$ and $|f\rangle$ are the initial and final states of the system respectively and V3 is the lowest order enharmonic part of the crystal potential. Higher order enharmonic terms lead to multi-phonon processes involving more than three phonons. These processes are considered too weak to strongly change the relaxation rate. Equation (1) requires one to evaluate the form of V3, the cubic enharmonic part of the crystal potential. Within an elastic continuum approach, V3 can be written as

$$V_3 = \frac{1}{3!}\int d^3r \sum_{lmn}\sum_{ijk} A_{ijk}^{lmn}\frac{\delta u_l}{\delta r_i}\frac{\delta u_m}{\delta r_j}\frac{\delta u_n}{\delta r_k}, \qquad (1)$$

For a three-dimensional continuum it can be readily shown that the displacement vector is of the form

$$\mathbf{u}(\mathbf{r}) = \frac{1}{\sqrt{V_0}}(-i)\sqrt{\frac{\hbar}{2\rho}}\sum_{\mathbf{qs}}\sqrt{\frac{1}{\omega(\mathbf{qs})}}\mathbf{e}_{\mathbf{qs}}(a^\dagger_{\mathbf{qs}} - a_{-\mathbf{qs}})e^{i\mathbf{q}\cdot\mathbf{r}} \qquad (2)$$

Where, p is the mass density per unit volume, s indicates the phonon branch and q is the wave vector. Vo is the volume of the material and aqs and $a^\dagger$ are the phonon creation and annihilation operators respectively. For a one-dimensional system, Eq. (2) is modified by Vo → Lo and p → p' where Lo is

the length of the nanostructure and p' is the mass per unit length. It is important to note here that the vectors, u, q and e are maintained irrespective of whether the system is one-, tow- or three-dimensional. Differentiating Eq. (2) with respect to r, and substituting into Eq. (2), the form of potential becomes

$$V_3 = \frac{1}{3!}\int d^3r \left(\frac{\hbar}{2V_0\rho}\right)^{3/2}\sum_{\mathbf{q}\mathbf{q}'\mathbf{q}''}\sum_{s,s',s''} A_{ijk}^{lmn}\sqrt{\frac{1}{\omega(\mathbf{qs})\omega(\mathbf{q}'s')\omega(\mathbf{q}''s'')}}\times q_i e^l_{\mathbf{qs}} q'_j e^m_{\mathbf{q}'s'} q''_k e^n_{\mathbf{q}''s''}(a^\dagger_{\mathbf{qs}} - a_{-\mathbf{qs}})(a^\dagger_{\mathbf{q}'s'} - a_{-\mathbf{q}'s'})\times (a^\dagger_{\mathbf{q}''s''} - a_{-\mathbf{q}''s''})e^{i((\mathbf{q}+\mathbf{q}'+\mathbf{q}'')\cdot\mathbf{r})}, \qquad (4)$$

for three-dimensional systems, where Q_z, Q'_z and Q''_z are the magnitudes of the wave vectors q, q', and q" respectively and e^l_{qs}, $e^m_{q's'}$ and $e^n_{q''s''}$ are the polarization vectors of the phonon mode, Similarly, for a one-dimensional system one obtains

$$V_3 = \int dr \left(\frac{\hbar}{2L_0\rho'}\right)^{3/2} \sum_{q,q',q''} \sum_{s,s',s''} A_{ijk}^{lmn} \sqrt{\frac{1}{\omega(\mathbf{qs})\omega(\mathbf{q's'})\omega(\mathbf{q''s''})}} \times q_i e^l_{\mathbf{qs}} q'_j e^m_{\mathbf{q's'}} q''_k e^n_{\mathbf{q''s''}} (a^\dagger_{\mathbf{qs}} - a_{-\mathbf{qs}})(a^\dagger_{\mathbf{q's'}} - a_{-\mathbf{q's'}}) \times (a^\dagger_{\mathbf{q''s''}} - a_{-\mathbf{q''s''}}) e^{i(\mathbf{q}+\mathbf{q'}+\mathbf{q''})\cdot\mathbf{r}} \quad (5)$$

It in now possible to solve the integration in Eqs. (4) and (5) using the Fourier theorem

$$\frac{1}{\mathcal{L}^D} \int d^D r e^{i(\mathbf{q}+\mathbf{q'}+\mathbf{q''})\cdot\mathbf{r}} = \delta_{\mathbf{q}+\mathbf{q'}+\mathbf{q''},\mathcal{G}} \quad (6)$$

where ς is the reciprocal lattice vector for Umklapp processes and ς = 0 for Normal processes. D is the number of dimensions. For one dimensional system L1 = Lo and for three dimensional systems L3 =Vo Using this identity, it is possible to rewrite Eq. (5) as

$$V_3 = \left(\frac{\hbar^3}{8L_0\rho'^3}\right)^{1/2} \sum_{q,q',q''} \sum_{s,s',s''} A_{ijk}^{lmn} \sqrt{\frac{1}{\omega(\mathbf{qs})\omega(\mathbf{q's'})\omega(\mathbf{q''s''})}} \times q_i e^l_{\mathbf{qs}} q'_j e^m_{\mathbf{q's'}} q''_k e^n_{\mathbf{q''s''}} (a^\dagger_{\mathbf{qs}} - a_{-\mathbf{qs}})(a^\dagger_{\mathbf{q's'}} - a_{-\mathbf{q's'}}) \times (a^\dagger_{\mathbf{q''s''}} - a_{-\mathbf{q''s''}}) \delta_{\mathbf{q}+\mathbf{q'}+\mathbf{q''},\mathcal{G}} \quad (7)$$

To simplify this expression further, one applies the following substitution to simplify A^{lmn}_{ijk}

$$A^{s,s',s''}_{q,q',q''} = \sum_{ijk} \sum_{lmn} e^l_{\mathbf{qs}} v_i e^m_{\mathbf{q's'}} v'_j e^n_{\mathbf{q''s''}} v''_k A^{lmn}_{ijk} \quad (8)$$

where V, V' V" are the unit vectors along q, q' and q" respectively.

1.1.2 Analytic model for relaxation rate in carbon nanotubes

For a qualitative analytic expression, it is necessary that one applies the linear Deye model to carbon nanotubes. As this is a simplistic model, for explaining trends and features of the relaxation rate of phonon modes undergoing three-phonon interactions, the effect of the optical modes shall be discarded immediately as their consideration should not change the form of the expressions derived. Thus, this leaves the acoustic branches TA,LA, and WA of the form ω_ϑ(Kz)= csKz wher cs is the group velocity of mode ϑ. To simplify this model further let m = 0 for all modes. Using this relation, one obtains the density of states for each of these modes as:

$$g(\omega,\vartheta) = \frac{L_0}{\pi C_s}$$

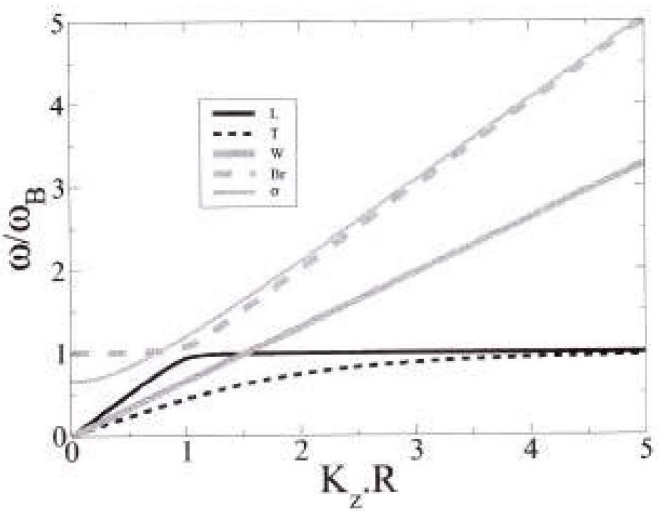

Figure 1: The phonon dispersion curves of the six lowest branches for a carbon nanotube of radius R. ω_B is the frequency of the breathing mode at the zone centre. Here the letter corresponds to the phonon branch: L = Longitudinal, T = (doubly degenerate) Transverse, W = Twist, Br = Breathing and σ = σ (the lowest non-zero mode).

Table 1: The allowed combinations of phonon polarization branches within the simple analytic model.

Phonon branch with velocity Cs1		Phonon branch with velocity Cs2 and Cs3
LA	↔	WA + TA
LA	↔	TA + WA
WA	↔	LA + TA
WA	↔	TA + LA
TA	↔	LA + WA
TA	↔	WA + LA

III. RESULTS

3.1 Lifetime of zone-center optical modes in carbon nan-tubes

For the feasibility of the study presented above calculations were performed for armchair (n, n) carbon nanotubes, with n ranging from 5 to 20. The nanotube radius r is related, for an (n,n) tube, to n by [illegible] where ac-c = 0.144 nm. It was assumed that the confined modes ([illegible]) and ([illegible]B) can decay into the four acoustic mode (the longitudinal L, doubly degenerate transverse T and the twist W).

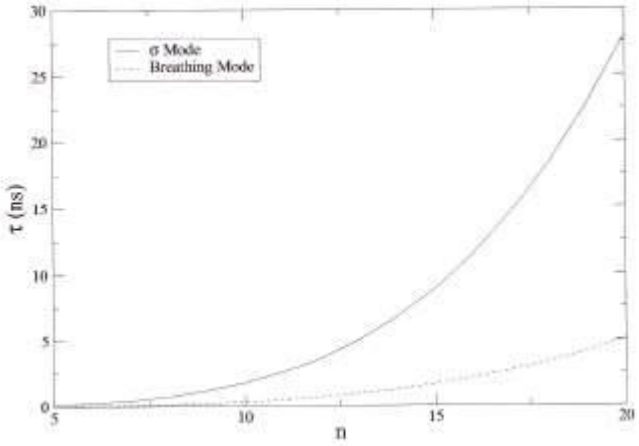

Figure 2: The variation of the lifetime of the lowest non-zero zone-centr confined mode and the breathing mode in (n,n) carbon nanotubes at 300 K. $\omega_B/(2\pi)$

The acoustic speeds for all n values are cL = 21.6 km/s, cT = 10.0 km/s, cW =14.5 km/s. For the (10,10) nanotube [illegible]=3.43 THz and=5.25 THz. For other sizes of the nanotubes both wq and wB scaleas 1/n. From Fig 2 one observes a steady increase in the lifetime of both modes with an increase in the nanotube radius. The Fig.3 increases linearly with temperature in the entire presented range which is what would be expected for the high temperature behavior of a phonon mode. This is due to the very low frequencies of these modes, making hw/kT much smaller that unity for all the temperatures considered. This can be contrasted with the intrinsic lifetime of the zone-centre optical modes in bulk diamond, which due to their high frequency shows a linear variation only above the Debye temperature.

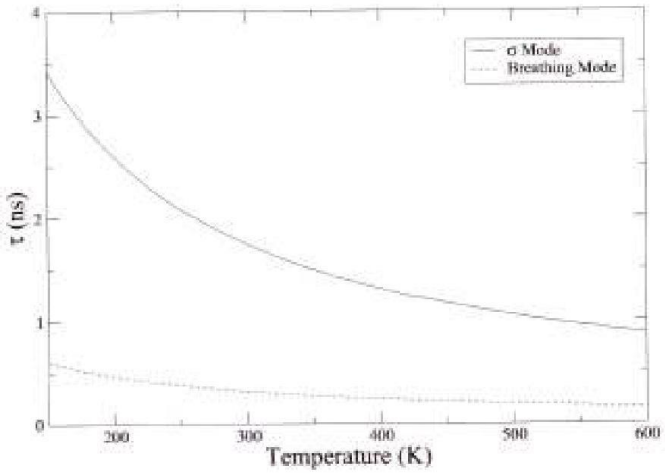

Figure 4: The lifetime of the lowest non-zero zone-centre confined mode and the breathing mode and the breathing mode as a function of temperature for a (10,10) carbon nanotube. $\omega_{\sigma}/2\pi$

While the trend in the variation of the lifetime of the two modes is correctly described by Figs. 3 and 4, the numerical results of the lifetimes are subject to the choice of the acoustic speeds and the frequencies of the modes.

Table 3: The frequencies of the lowest non-zero zone- centre confined mode and the acoustic speeds of the longitudinal and doubly transverse modes for a silicon nanowire of thickness d.

d (nm)	cL (km/s)	cT (km/s)	$\omega_{\sigma/2\pi}$ (THz)
0.543	24.43	20.27	4.737
1.086	11.86	8.50	3.199
1.629	10.69	7.58	2.628
2.172	9.88	6.67	2.126
2.715	9.10	6.50	1.782
3.258	8.91	6.18	1.520
3.801	8.71	6.11	1.344

is that these low lying optical modes in carbon nanotubes have lifetimes comparable with those of acoustic modes in bulk materials.

3.2 Lifetime of zone-center optical modes in silicon nanowires
Calculations were made for square thin silicon nanowires whose cross section area varied in size from 0.543 nm × 0.543 nm to 3.801 nm × 3.801 nm. The frequency [illegible] and the speeds of the acoustic modes (longitudinal and doubly transverse) obtained from above are given in Table 3. Except for the ultrathin wire (thickness 0.543 nm), the lifetime of the [illegible] mode in rouse with wire thickens, an shown in Fig-5. By Wmpitrinon the life time of W6 mode in the nanowire changes much more slowly with width than either of the two optical modes in the carbon nanotube. The calculations show that, at room temperature for the nanowire with thickness of 2.7 nm, the lifetime of the [illegible] mode is comparable to the lifetime.

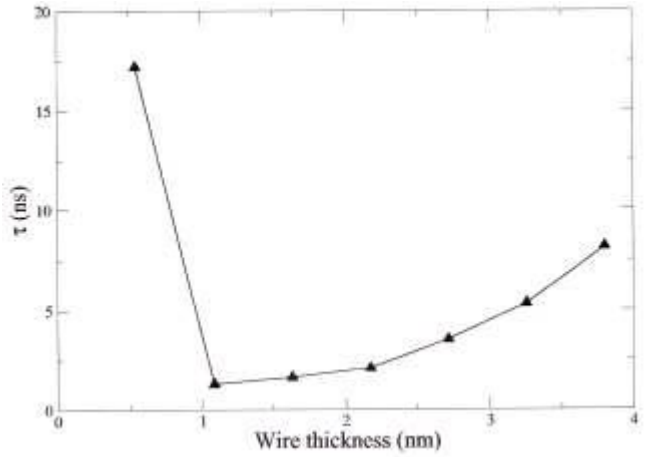

Figure 5: The variation of the lifetime of the lowest non-zero zone-center confined mode with the thickness of the wire at 300 K.

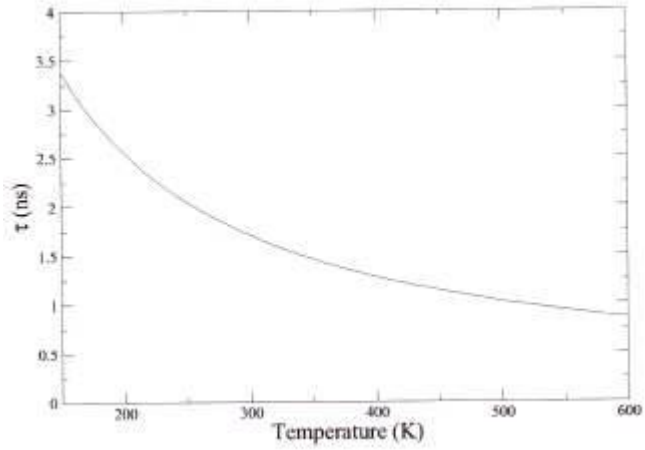

Figure 6: The lifetime of the lowest non-zero zone-center confined mode as a function of temperature for a nanowire of thickness 2.172 nm.

3.3. The (10,10) Nanotube at Room Temperature

3.3.1 Frequency variation

The phonon dispersion curves for the continuum theory, are shown in Fig .2 Fig. 2 Figure 7 (a)displays the total lifetime of different phonon modes undergoing three-phonon processes for the (10,10) nanotube, at 300 K as a function of frequency. The figures showing that the high temperature behavior of these modes can approximated and explained very effectively with this simple expression. Also, the cut off points in the relaxation rate of these modes are direct results of the phonon dispersion curves of the corresponding modes. For example, above the frequency [illegible] B there are no valid frequencies for real KZ values for the longitudinal and transverse modes. Figure 7 (b) displays the results of considering only Umklapp processes involving only the four acoustic branches (LA, doubly degenerate TA, and WA) This enables a comparison of these results (based upon the method presented in section 3.3) with those of Xiao et al. The results indicate that the relaxation rate of the acoustic modes is much greater than those presented by Xiao et al. The author is unable to understand this difference except to speculate that their enharmonic potential is much weaker that that applied there and does not include one-dimensional effects which are vital. However, the results of the previous section.

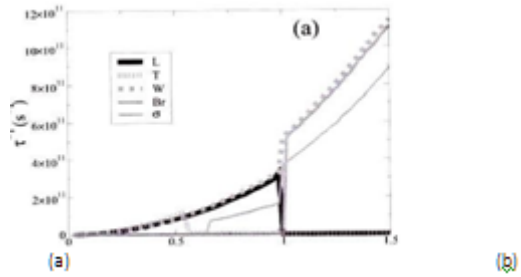

Figure 7: The inverse relaxation time of different phonon modes as a function of frequency [illegible] for a (10,10) carbon nanotube at 300 K for: (a) [illegible] and B modes with Normal processes included; (b) LA, TA and WA modes only undergoing Umklsapp processes. [illegible]B is the frequency of the breathing mode at the zone center. Here the letter corresponds to the mode (LA= Longitudinal. TA= (doubly degenerate) Transverse, WA=Twist, B= Breathing and [illegible] (the lowest non-zero mode)).

Parison of the relaxation rates with bulk diamond (which has a comparable thermal conductivity) shows good agreement and indicates that these results for the nanotube re more acceptable and correct. The general form of the frequency dependency in the low frequency region is in good agreement with Xiao et al. The difference between the results presented in Figs. 7 (a) and

(b) is due to the inclusion of two factors: (i) the breathing a 6 modes, and (ii) Normal processes. However, the main difference between Fig. 7 (a) and (b) arises due to the inclusion of the two optical modes, which has resulted in almost doubling of the total relaxation rate of the longitudinal and twist modes. The second point is less important because the contribution from Normal processes at room temperature is much smaller.

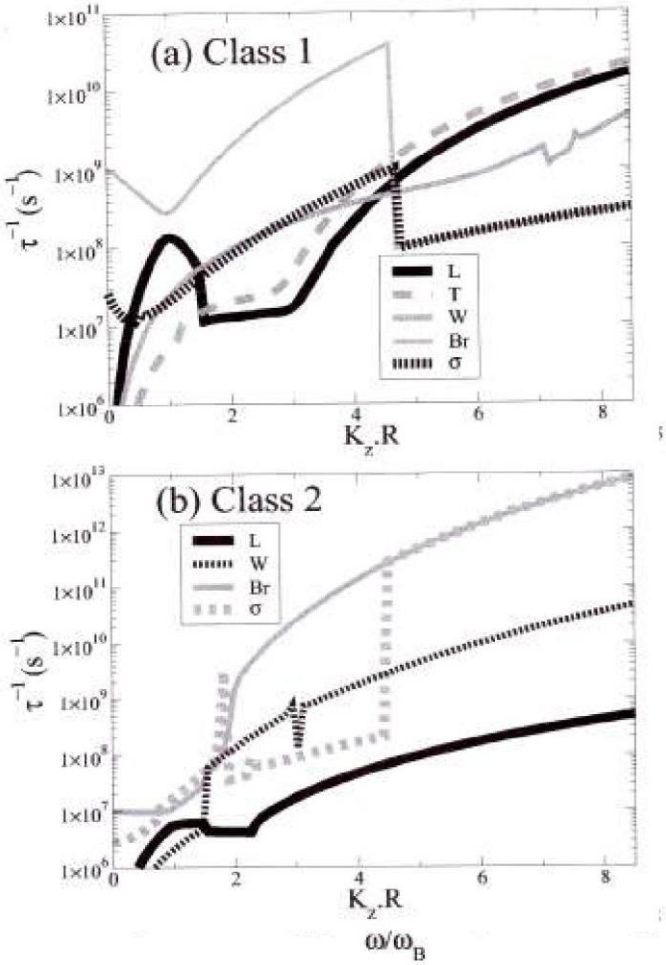

Figure 8 (a-b) shows that the relaxation rates of both the LA and the WA modes also varies with frequency as $T^{-1} \propto \omega^2$ for the range shown.

Table 5: Relaxation rates of different phonon modes undergoing various processes for the (10,10) nanotube at 300 K. The maximum value for KZ.R is 8.66.

Normal or Umklapp	K_zR	Branch	Class 1 relaxation rate (s^{-1})	Class 2 relaxation rate (s^{-1})
N	1	LA	0.136×10^{9}	0.554×10^{7}
N	1	B	0.283×10^{9}	0.110×10^{8}
N	1	TA	0.257×10^{7}	N/A
N	1	WA	0.246×10^{8}	0.212×10^{7}
N	7.5	LA	0.926×10^{10}	0.335×10^{9}
N	7.5	B	0.236×10^{9}	0.335×10^{9}
N	7.5	σ	0.237×10^{9}	0.426×10^{13}
U	1	LA	0.270×10^{12}	N/A
U	1	B	0.346×10^{12}	0.224×10^{12}
U	1	TA	0.390×10^{11}	N/A
U	1	WA	0.144×10^{12}	N/A
U	7.5	LA	N/A	0.764×10^{9}
U	7.5	B	0.797×10^{13}	0.675×10^{13}
U	7.5	σ	0.782×10^{13}	0.683×10^{13}

IV. CONCLUSION

Lifetimes of low-lying confined phonon modes in carbon nanotubes and silicon nanowires have been estimate theoretically using a three-dimensional approach. It is found that these modes are very, long-lived, with lifetimes of the order of nanoseconds and are comparable with bulk acoustic modes. These lifetimes are found to increase with size but decrease linearly with temperature above 150 K. An exception to the trend is the ultrathin silicon nanowire of thickness 0.543 nm, which shows an increase in the lifetime of the lowest confined mode, which is an order of magnitude larger than that expected from extrapolation of the results for other thicknesses. From these results one concludes that in the following analysis of the relaxation rate of phonon modes in carbon nanotubes, the two low lying optical modes, wB and w6 and their corresponding frequency branches must be considered. Also, there results show that for any calculation of the relaxation rate of silicon nanowires, these modes must be included.

REFERENCES

[1] Particle Data Group Collaboration (K. A. Olive et al.), Review of Particle Physics, Chin. Phys. C38 (2014) 090001.

[2] ATLAS Collaboration, Observation of a new particle in the search for the Standard Model Higgs boson with the ATLAS detector at the LHC, Phys. Lett. B716 (2012) 1–29, arXiv:1207.7214 [hep-ex].

[3] CMS Collaboration, Observation of a new boson at a mass of 125 GeV with the CMS experiment at the LHC, Phys. Lett. B716 (2012) 30–61, arXiv:1207.7235 [hep-ex].

[4] ATLAS and CMS Collaborations, Combined Measurement of the Higgs Boson Mass in pp Collisions at √ s = 7 and 8 TeV with the ATLAS and CMS Experiments, Phys. Rev. Lett. 114 (2015) 191803, arXiv:1503.07589 [hep-ex].
[5] ATLAS, CDF, CMS and D0 Collaborations, First combination of Tevatron and LHC measurements of the top-quark mass, arXiv:1403.4427 [hep-ex].
[6] W. Cottingham and D. Greenwood, An Introduction to the Standard Model of Particle Physics. Cambridge University Press, 2007.
[7] R. Feynman, Space - time approach to quantum electrodynamics, Phys. Rev. 76 (1949) 769–789.
[8] R. Feynman, Mathematical formulation of the quantum theory of electromagnetic interaction, Phys. Rev. 80 (1950) 440–457.
[9] J. S. Schwinger, On Quantum electrodynamics and the magnetic moment of the electron, Phys. Rev. 73 (1948) 416–417.
[10] S. Tomonaga, On a relativistically invariant formulation of the quantum theory of wave fields, Prog. Theor. Phys. 1 (1946) 27–42. 57 58 Bibliography
[11] L3 Collaboration (P. Achard et al.), Measurement of the running of the electromagnetic coupling at large momentum-transfer at LEP, Phys. Lett. B623 (2005) 26–36, arXiv:hep-ex/0507078 [hep-ex].
[12] P. J. Mohr, B. N. Taylor and D. B. Newell, CODATA recommended values of the fundamental physical constants: 2006, Rev. Mod. Phys. 80 (2008) 633–730, arXiv:0801.0028 [physics.atom-ph].
[13] F. Tkachov, A Contribution to the history of quarks: Boris Struminsky's 1965 JINR publication, arXiv:0904.0343 [physics.hist-ph].
[14] F. Mandl and G. Shaw, Quantum field theory. Wiley, 1993.
[15] D. J. Gross and F. Wilczek, Ultraviolet Behavior of Nonabelian Gauge Theories, Phys. Rev. Lett. 30 (1973) 1343–1346.
[16] H. D. Politzer, Reliable Perturbative Results for Strong Interactions, Phys. Rev. Lett. 30 (1973) 1346–1349.
[17] R. P. Feynman, Very high-energy collisions of hadrons, Phys. Rev. Lett. 23 (1969) 1415–1417.
[18] J. Bjorken, Asymptotic Sum Rules at Infinite Momentum, Phys. Rev. 179 (1969) 1547–1553.
[19] H1 and ZEUS Collaborations (F. D. Aaron et al.), Combined Measurement and QCD Analysis of the Inclusive e+- p Scattering Cross Sections at HERA, JHEP 1001 (2010) 109, arXiv:0911.0884 [hep-ex].
[20] A. Martin et al., Parton distributions for the LHC, Eur. Phys. J. C63 (2009) 189–285, arXiv:0901.0002 [hep-ph].
[21] H.-L. Lai et al., New parton distributions for collider physics, Phys. Rev. D82 (2010) 074024, arXiv:1007.2241 [hep-ph].
[22] NNPDF Collaboration (R. D. Ball et al.), Parton distributions for the LHC Run II, JHEP 1504 (2015) 040, arXiv:1410.8849 [hep-ph].
[23] V. Gribov and L. Lipatov, Deep inelastic e p scattering in perturbation theory, Sov. J. Nucl. Phys. 15 (1972) 438–450.
[24] G. Altarelli and G. Parisi, Asymptotic Freedom in Parton Language, Nucl. Phys. B126 (1977) 298.
[25] Y. L. Dokshitzer, Calculation of the Structure Functions for Deep Inelastic Scattering and e+ e- Annihilation by Perturbation Theory in Quantum Chromodynamics., Sov. Phys. JETP 46 (1977) 641–653.